UNCLASSIFIED

SECURITY CLASSIFICATION OF THIS PAGE (When Data Entered)

LEVEL II

REPORT DOCUMENTATION PAGE

READ INSTRUCTIONS BEFORE COMPLETING FORM

1. REPORT NUMBER	2. GOVT ACCESSION NO.	3. RECIPIENT'S CATALOG NUMBER
AFOSR-TR-81-0283	AD-A096 945	

4. TITLE (and Subtitle)	5. TYPE OF REPORT & PERIOD COVERED
CRUSTAL AND UPPER MANTLE VELOCITY AND Q OF MAINLAND CHINA A079659	Interim
	6. PERFORMING ORG. REPORT NUMBER
7. AUTHOR(s)	8. CONTRACT OR GRANT NUMBER(s)
Ta-liang Teng	F49620-76-C-0010
9. PERFORMING ORGANIZATION NAME AND ADDRESS	10. PROGRAM ELEMENT, PROJECT, TASK AREA & WORK UNIT NUMBERS
Geophysics Laboratory University of Southern California Los Angeles, CA 90007	62701E 3291-21
11. CONTROLLING OFFICE NAME AND ADDRESS	12. REPORT DATE
AFOSR/ NP Bolling AFB, DC 20332	Sep 1980
	13. NUMBER OF PAGES 26
14. MONITORING AGENCY NAME & ADDRESS(if different from Controlling Office)	15. SECURITY CLASS. (of this report) unclassified
	15a. DECLASSIFICATION DOWNGRADING SCHEDULE

16. DISTRIBUTION STATEMENT (of this Report)

Approved for public release; distribution unlimited.

DTIC ELECTE MAR 27 1981 S D E

17. DISTRIBUTION STATEMENT (of the abstract entered in Block 20, if different from Report)

18. SUPPLEMENTARY NOTES

19. KEY WORDS (Continue on reverse side if necessary and identify by block number)

20. ABSTRACT (Continue on reverse side if necessary and identify by block number)

Multiple-filter technique and generalized linear inversion are applied to group velocity data derived from properly rotated three-component digital surface waves from Seismological Research Observatory stations. Repeated group velocity measurements over the same paths were made possible by using larger aftershocks of several great (M greater than 7) earthquakes that recently occurred in China. Specific attention is paid to the crustal and upper mantle structure of the Qinghai-Xizang plateau and its comparison with those of neighboring tectonic provinces. The results demonstrate the strong lateral heterogeneity in the →next page

DD FORM 1 JAN 73 1473

UNCLASSIFIED

SECURITY CLASSIFICATION OF THIS PAGE (When Data Entered)

AD A096945

DTIC FILE COPY

crust and upper mantle of the Chinese mainland. A particularly thick crust and an upper mantle of relatively low velocity are found underlying the Qinghai-Xizang plateau that corroborates the continental collision between India and Eurasia.

Accession For
NTIS GRA&I X
DTIC TAB
Unannounced
Justification
By
Distribution/
Availability Codes
Dist | Avail and/or Special
A

AFOSR-TR-81-0283

SEMI-ANNUAL TECHNICAL REPORT

submitted to the

Air Force Office of Scientific Research

by the

Geophysics Laboratory
University of Southern California

Contractor:	University of Southern California
Effective Date of Contract:	July 2, 1976
Amount of Contract:	$143,003
Contract Number:	F49620-76-C-0010, ARPA Order-3291
Principal Investigator:	Ta-liang Teng Professor of Geophysics (213) 743-6124
Program Manager:	Bill Best
Title:	CRUSTAL AND UPPER MANTLE VELOCITY AND Q OF MAINLAND CHINA
Sponsored by:	Advanced Research Projects Agency (DOD) ARPA Order No. 3291
Date of Report:	Sep[redacted]80

12 28

16 3291

17 21

S/C 408856

Approved for public release;
distribution unlimited.

81 3 27 014

AIR FORCE OFFICE OF SCIENTIFIC RESEARCH (AFSC)
NOTICE OF TRANSMITTAL TO DDC
This technical report has been reviewed and is approved for public release IAW AFR 190-12 (7b).
Distribution is unlimited.
A. D. BLOSE
Technical Information Officer

CRUSTAL AND UPPER MANTLE STRUCTURE OF QINGHAI-XIZANG PLATEAU AND ITS SURROUNDING AREA

Ta-liang Teng
(Department of Geological Sciences,
University of Southern California,
Los Angeles, California, USA 90007)

ABSTRACT

Multiple-filter technique and generalized linear inversion are applied to group velocity data derived from properly rotated three-component digital surface waves from Seismological Research Observatory stations. Repeated group velocity measurements over the same paths were made possible by using large aftershocks of several great (M > 7) earthquakes that recently occurred in China. Specific attention is paid to the crustal and upper mantle structure of the Qinghai-Xizang plateau and its comparison with those of neighboring tectonic provinces. The results demonstrate the strong lateral heterogeneity in the crust and upper mantle of the Chinese mainland. A particularly thick crust and an upper mantle of relatively low velocity are found underlying the Qinghai-Xizang plateau that corroborates the continental collision between India and Eurasia.

INTRODUCTION

One of the most outstanding landscapes of grandiose scale on the earth, the Himalayas and the Qinghai-Xizang plateau, has long held the interest of earth scientists. Many recognized that in this vast region, having the highest as well as the youngest mountain ranges in the world, lies an important key to a major tectonic process that took place in the recent past. Besides the surface expressions, the plate collision between India and Eurasia must have produced fundamental modifications in the crust and upper mantle underlying this giant plateau. There is great interest to delineate these modifications. A detailed delineation will undoubtedly provide useful constraints on models proposed for the collision process. Among geophysical tools, surface wave dispersion analysis is one of the most effective means for the crustal and upper-mantle delineations. Knowledge of the crustal thickness and velocity structure under the Qinghai-Xizang plateau from other surface wave dispersion studies is limited. Early works by Stonely[1], Tandon and Chandhury[2], Sara[3], Zeng et al.[4], Gupta and Narain[5], and Negi and Singh[6] have given some gross descriptions of the earth's crust underneath this plateau. Most of their results generally represent the average crustal structure over long surface wave paths through which the plateau only accounts for a short segment. More detailed works were carried out by Bird and Toksöz[7], Tung[8], and Chun and Yoshii[9]. Their results were among the first to give information on the plateau's layering crust.

In order to have a surface wave study that more directly reflects the crustal and upper mantle structure of a tectonic province, it is important to obtain as close to pure-path dispersion data as possible. Moreover, re-

peated dispersion measurements over the same surface wave path are desirable to improve the data reliability. Our work begins by tectonically dividing China into four major provinces here referred to as subplates (Fig. 1). Each subplate has a similar tectonic past, therefore, it can be considered to a first approximation as a single tectonic unit over which the lateral change of crustal and upper mantle structure is relatively small. Among the four subdivisions in figure 1, the Qinghai-Xizang plateau forms a subplate by itself, and this paper shall concentrate on the derivation of its crustal and upper mantle structure. To obtain pure-path dispersion data, we take advantage of (1) several large ($M > 7$) earthquakes that have occurred near the boundaries of these subplates and (2) two high-quality Seismological Research Observatory (SRO) stations located near boundaries of these subplates. Therefore, a reasonable pure-path configuration is closely approximated. We note that tectonically the western extension of the Qinghai-Xizang subplate should also include northern Pakistan and Afghanistan, for the entire orogeny belt was formed during the collision process. Besides the two paths crossing the Qinghai-Xizang plateau, we also studied three other paths that sample the surrounding three subplates so that a comparative analysis can be made to obtain information on lateral variations of crustal and upper mantle structure in China.

DATA AND METHOD

Table 1 gives all earthquake sources used. They are large aftershocks of the three damaging earthquakes that occurred in China in 1976. A number of sources are used for each path in order to obtain an estimate on the uncertainty of the observed dispersion data. All events in this study were recorded at two SRO stations located in Mashad, Iran (MAIO) and Taipei, Taiwan (TATO). SRO stations operate at high gain, thus lowering the detection threshold for seismic events and making small-magnitude events ($M \sim 5$) useful for long- and short-period surface wave dispersion analysis. Using smaller events would also avoid the difficulty in dispersion analysis often caused by large multiple and propagating sources. Since the SRO data are digitally recorded, pure Love and Raleigh waves are conveniently obtained by rotating the data coordinates. An example of a seismic event, before and after rotation, is given in figures 2 and 3. Surface wave data are windowed and subjected to a multiple-filtering analysis. A typical contoured result of the relative amplitude of surface wave energy arrivals over the path Yunnan-Mashad for both vertical and radial Rayleigh waves is shown in figures 4 and 5. The dots in these figures represent the average group velocities over the filter band. Both fundamental mode and the first higher mode energies are clearly present. Dispersion data extracted from these contour plots for the two paths through the Qinghai-Xizang subplate are given in figures 6-8. Along the path Sichuan-Mashad, five events each with two (vertical and radial) Rayleigh components are used to obtain the observed dispersion data given in figure 9. Thus in figure 9, every observed dispersion data point is the average of ten independent measurements. The standard errors as a result of these repeated measurements range from 3-5%. The averaged dispersion data for the path Yunnan-Mashad are given in figure 10. For the purposes of comparison, three other paths have also been studied. Their averaged observed dispersion data are given in figures 11-14. A visual examination of these observed dispersion data immediately reveals that those paths traversing through the Qinghai-Xizang plateau give substantially lower group velocity values. This anomalously low group velocity extends to a period as long as

80 s, suggesting that the anomalous structure of the Qinghai-Xizang plateau extends down to the upper mantle.

A generalized linear inversion method first introduced by Backus and Gilbert[10] is applied to the observed dispersion data. Detailed descriptions of this method have been presented by Jackson[11], Wiggins[12], and Crosson[13]. The basic logic of the inversion theory and some experience in its numerical applications can be found in Pines et al.[14]. Initial models used for the inversion were based on the results of Tung[8]. The data were first inverted for both shear velocity and density. During the inversion process, large instabilities of the density parameter were found in the crust. This was corrected by changing the starting models to ones that more closely approximated the dispersion data, and at the same time compressional velocity was also included as an inversion parameter. As discussed by Wiggins[12], Der et al.[15], and Jackson and Burkhard[16], the partial derivatives for shear velocity are larger than those for compressional velocity or density. Therefore, the resolution for shear velocity is considerably better than for the other two parameters.

RESULTS AND DISCUSSION

Upon application of a generalized linear inversion to the observed dispersion data (shown by open squares in figures 9-14), we have obtained the best-fit models corresponding to each path with theoretical group velocities for each of these models given as open circles in the respective figures. For the two paths crossing the Qinghai-Xizang plateau, the first higher mode data are available and they were also entered into the inversion process. Love waves were not used in the inversion due to the absence of amplitude maxima in the dispersion curves between 30 s and 60 s. Earlier studies by Thatcher and Brune[17] and James[18] have discussed the problem of interference of Love waves crossing inhomogeneous media. Tung[8] attributed this problem on the Qinghai-Xizang plateau to Love waves following a non-least time path. A possible structural implication is that there may be structures along the path corresponding to wavelengths of Love waves, causing part of the wave energy to travel along a non-least time path with slower velocities. Resulting models are labeled SM1 for the Sichuan-Mashad path, and YM1 for the Yunnan-Mashad path. Numerical values of the two models are given in Tables 2 and 3. In the inversion process, the compressional velocity and the density values were practically unchanged as they are not very sensitive parameters for the group velocity. Initial and final values of the shear velocity are tabulated to show the changes as required by the data. To compare the crustal and upper mantle structure of the Qinghai-Xizang plateau with its surrounding regions, we have a summary plot given in figure 15 where the shear velocity structures of the models SM1 and YM1 are shown together with three other models resulting from the dispersion data along the three other paths: TM1 for Tangshan-Mashad, TT1 for Tangshan-Taipei, and SC1 for Sichuan-Taipei. The comparison in figure 15 shows a distinctly thick crust for the Qinghai-Xizang plateau, with lower crust extending to a depth of about 70 km. From the width of the resolving kernels it is only possible to resolve layers of 10-15 km in the upper crust, 15-20 km in the middle crust, and 25-30 km in the lower crust. Resolution in the mantle is poor, a low-velocity layer in the upper mantle can only be inferred. Additional data for periods much longer than 120 s and good Love waves as well as higher mode data would significantly increase the resolving power of the upper mantle

structure. The shear wave velocity structure for both paths crossing the Tibetan plateau is similar. A 70 km thick crust may be broken into four layers. The first layer has shear velocities that range between 2.87 and 3.06 km/s, suggesting a layer approximately 15 km thick of partly sedimentary origin. Tung[8] and Mu et al.[19] discussed the existence of thick sedimentary layers in the Mount Jolmo Langma region of the Himalayas. Both Birch[20] and Simmons[21] reported shear velocities for sedimentary rocks at 10- to 15-km depth of approximately 3.00-3.08 km/s. A second layer has shear wave velocities ranging from 3.20 to 3.40 km/s and is approximately 15 km thick, suggesting a layer of granitic or equivalent composition. A third layer has shear velocities between 3.40 and 3.70 km/s is approximately 15-20 km thick, and also seems to consist of granite. For comparison, Birch and Bancroft[22], Birch[20], and Simmons[21] reported shear velocities for granite under 3-5 kbars of pressure of 3.45-3.70 km/s. Simmons reported that granite with a shear wave velocity of 3.79 km/s at pressures of 10 kbars. The fourth layer with shear wave velocities between 3.85 and 3.95 km/s corresponds to granite at pressures of approximately 20 kbars, which would correspond to depths of 60-70 km.

The dispersion curves and shear wave velocity profile for the Tibetan plateau are in agreement with those values presented by Tung[8] and Bird and Toksöz[7]. Chun and Yoshiii[9], using Rayleigh and Love waves for many different paths across the Qinghai-Xizang pleateau, reported a crustal thickness of approximately 70 km and observed a velocity reversal in the middle crust. Owing to a 15- to 20-km resolution in the middle crust it is doubtful a velocity reversal could be observed for data over the two paths presented.

Because of the small amount of information derived from inverting Rayleigh waves in the upper mantle, the above structural conclusions are only tentative. The upper mantle shear velocities are lower than either the Gutenburg earth model or the Canadian Shield. The velocity at the top of the mantle is approximately 4.4 km/s, with indications of a low-velocity layer at about 90-km depth. Since the low-velocity layer can only be inferred, the existence of extremely low velocities of 4.1 km/s is tentative. Low shear velocities in the upper mantle suggests a high degree of partial melting and a low resistance to deformation, Anderson et al.[23]

References

(1) Stonely, R., Rayleigh waves in a medium with two surface layers: Mon. Nat. Roy. Astron. Soc. Geophys. Supp. 7, pp. 71-75 (1955).

(2) Tandon, A. N., and Chandhury, H. M., Seismic waves from high yield atmospheric explosions: Ind. J. Met. Geophys. 14, pp. 283-301 (1963)

(3) Sara, B. P., M_2 or first shear mode continental Rayleigh waves from Russian nuclear explosion of 30 October 1961: Ind. J. Mt. Geophys. 16, pp. 270-280 (1965).

(4) Zeng, J. S. and Sung, Z. A., Phase velocity of Rayleigh waves in China: Acta Geophysica Sinica 12, no. 2, pp. 148-165 (1963).

(5) Gupta, H. K. and Narain, H., Crustal structure in the Himalayan and Tibetan plateau region from surface wave dispersion: Bull. Seism. Soc. Am., v. 57, no. 2, pp. 235-248 (1967).

(6) Negi, J. G. and Singh, V. P., Love wave dispersion analysis for crustal structure of laterally inhomogeneous Himalayas: Bull. Seism. Soc. Am., v. 63, no. 3, pp. 1163-1172 (1973).

(7) Bird, P. and Toksöz, M. N., Strong attenuation of Rayleigh waves in Tibet: Nature, V266, pp. 163-165 (1977).

(8) Tung, J. P., The surface wave study of crustal and upper mantle structure of Mainland China: Ph.D. dissertation, University of Southern California, 248 pp. (1974).

(9) Chun, K. Y. and Yoshii, Crustal structure of the Tibetan pleateau: A surface wave study by a moving window analysis: Bull. Seism. Soc. Am., v. 67, pp. 735-750 (1977).

(10) Backus, G. and Gilbert, F., Uniqueness in the inversion of inaccurate gross Earth data: Phil. Trans. Roy. Soc. (London), Ser. A266, pp. 123-192 (1970).

(11) Jackson, D. D., Interpretation of inaccurate, insufficient, and inconsistent data: Geophys. J. Roy. Astron. Soc. 28, pp. 97-109 (1972).

(12) Wiggins, R. A., The general linear inverse problems: Implications of surface waves and free oscillations for Earth structure: Rev. Geophys. Space Phys. 10, pp. 251-285 (1972).

(13) Crossen, R. S., Crustal structure modeling of earthquake data 1, simultaneous least squares estimation of hypocenter: J. Geophys. Res. 81, pp. 3030-3046 (1976).

(14) Pines, I., Teng, T. L., Rosenthal, R., and Alexander, S. S., A surface wave dispersion study of the crustal and upper mantle structure of China, J. Geophys. Res., vol. 85, pp. 3829-3844 (1980).

(15) Der, Z., Masse, R. and Landisman, M., Effects of observational errors on the resolution of surface waves at intermediate distances: J. Geophys. Res. 75, pp. 3399-3409 (1970).

(16) Jackson, D. D. and Burkhard, N. R., Density and surface wave inversions: Geophys. Res. Let. v. 3, no. 11, pp. 637-638 (1976).

(17) Thatcher, W. and Bruen, J. N., Higher mode interference and observed anomalous apparent Love wave velocities: J. Geophys. Res. 74, pp. 6603-6611 (1969).

(18) James, D. E., Anomalous Love wave phase velocities: J. Geophys. Res. 76, pp. 2077-2083 (1971).

(19) Mu, E. Z., Yin, J. X., Wen, S. X., Wang, Y. G. and Zhang, G. G., Stratigraphy of the Mount Jolmo Lunga region in Southern Tibet: Chinese Scientia Geologica Sinica, no. 1, pp. 13-25 (1973).

(20) Birch, F., Some geophysical applications of high pressure research in solids under pressure: edited by W. Paul and D. M. Warschauer; McGraw-Hill Book Company, New York (1963).

(21) Simmons, G., Velocity of shear waves in rocks to 10 kilobars: J. Geophys. Res. 69, no. 6, p. 1123 (1964).
(22) Birch, F., and Bancroft, D., The effect of pressure on the rigidity of rocks: J. Geol., 46, pp. 59-83 113-141 (1938).
(23) Anderson, D. L., Sammis, C. and Jordan, T., Composition of the mantle and core, the nature of the solid Earth: Edited by E. L. Robertson, McGraw Hill, p. 677 (1972).

TABLE 1. Pertinent Earthquakes Information Used in this Study

Location	Origin Time*	Station	M	Wave Type	Component	Path	Distance, km
32.8°N, 104.2°E Sichuan	Aug. 16, 1976 1406:45.9	MAIO	6.1	Rayleigh	vertical radial	Sichuan-Mashad	4080
32.9°N, 104.2°E, Sichuan	Aug. 19, 1976 1249:47.7	MAIO	5.4	Rayleigh	vertical radial	Sichuan-Mashad	4078
32.8°N, 104.2°E, Sichuan	Aug. 21, 1976 2149:54.2	MAIO	6.1	Rayleigh	vertical radial	Sichuan-Mashad	4095
32.5°N, 104.2°E, Sichuan	Aug. 23, 1976 0330:7.6	MAIO	6.2	Rayleigh	vertical radial	Sichuan-Mashad	4088
32.5°N, 104.2°E, Sichuan	Sept. 1, 1976 0106:51.8	MAIO	5.1	Rayleigh	vertical radial	Sichuan-Mashad	4090
24.3°N, 98.6°E, Yunnan	May 31, 1976 0508:28.5	MAIO	5.5	Rayleigh	vertical radial	Yunnan-Mashad	3956
24.2°N, 98.7°E, Yunnan	July 3, 1976 1633:23.1	MAIO	5.3	Rayleigh	vertical radial	Yunnan-Mashad	3967
39.8°N, 118.6°E, NE China	July 28, 1976 1535:55.3	TATO	5.4	Rayleigh Love	vertical radial transverse	Tangshan-Taipei	1661
39.8°N, 118.9°E, NE China	July 30, 1976 2123:13.8	TATO	5.4	Rayleigh Love	vertical radial transverse	Tangshan-Taipei	1670
39.6°N, 117.8°E, NE China	Aug. 1, 1976 2053:53.6	TATO	4.6	Rayleigh Love	vertical radial transverse	Tangshan-Taipei	1656
39.9°N, 118.8°E, NE China	Sept. 6, 1976 1702:01.5	TATO	4.8	Rayleigh	vertical	Tangshan-Taipei	1672
39.9°N, 118.0°E, NE China	July 29, 1976 0101:04.1	MAIO	5.1	Rayleigh Love	vertical transverse	Tangshan-Mashad	5119
39.8°N, 117.8°E, NE China	July 30, 1976 2123:13.8	MAIO	5.4	Love	transverse	Tangshan-Mashad	5072
39.6°N, 117.9°E, NE China	Aug. 2, 1976 0916:00.5	MAIO	4.4	Rayleigh	vertical	Tangshan-Mashad	5053
39.7°N, 118.5°E, NE China	Aug. 8, 1976 0109:12.4	MAIO	4.9	Rayleigh Love	vertical transverse	Tangshan-Mashad	5100

TABLE 1. Pertinent Earthquakes Information Used in this Study (Continued)

Location	Origin Time*	Station	M	Wave Type	Component	Path	Distance km
40.2°N, 118.9°E, NE China	Aug. 8, 1976 2241:34.3	MAIO	5.1	Rayleigh	vertical	Tangshan-Mashad	5118
39.6°N, 118.5°E, NE China	Aug. 14, 1976 1602:44.5	MAIO	4.7	Rayleigh Love	vertical transverse	Tangshan-Mashad	5103
32.9°N, 104.2°E, Sichuan	Aug. 19, 1976 1249:47.7	TATO	5.4	Rayleigh	vertical	Sichuan-Taipei	1902
33.0°N, 104.2°E, Sichuan	Aug. 22, 1976 1319:53.0	TATO	4.7	Rayleigh	vertical	Sichuan-Taipei	1884
32.5°N, 104.2°E, Sichuan	Sept. 1, 1976 0106:51.8	TATO	5.1	Rayleigh Love	vertical transverse	Sichuan-Taipei	1886
28.0°N, 100.0°E, Sichuan	Sept. 3, 1976 0957:28.5	TATO	5.2	Love	transverse	Sichuan-Taipei	1854

TABLE 2. Model Fit for Path Szechwan-Mashad

Layer	H, km	α, km/s	β,* km/s	ρ, g/cm	β,† km/s
1	15	5.55	2.80	2.70	3.06
2	15	5.60	3.20	2.90	3.28
3	25	6.40	3.30	3.00	3.67
4	20	6.60	3.80	3.10	3.98
5	25	7.50	4.45	3.30	4.39
6	25	7.20	4.20	3.35	4.31
7	25	7.20	4.10	3.36	4.18
8	25	7.20	4.20	3.37	4.21

*Initial model.
†Final model.

TABLE 3. Model Fit for Path Yunnan-Mashad

Layer	h, km	α, km/s	β,* km/s	p, g/cm	β,† km/s
1	10	5.50	2.80	2.70	2.91
2	10	5.60	3.10	2.90	3.29
3	10	5.65	3.20	2.92	3.40
4	10	6.25	3.30	3.00	3.56
5	15	6.45	3.40	3.05	3.54
6	15	6.60	3.80	3.10	3.90
7	20	7.45	4.45	3.30	4.44
8	20	7.20	4.20	3.34	4.19
9	25	7.20	4.15	3.35	4.10
10	25	7.20	4.15	3.36	4.10
11	25	7.20	4.20	3.37	4.15

*Initial model.
†Final model.

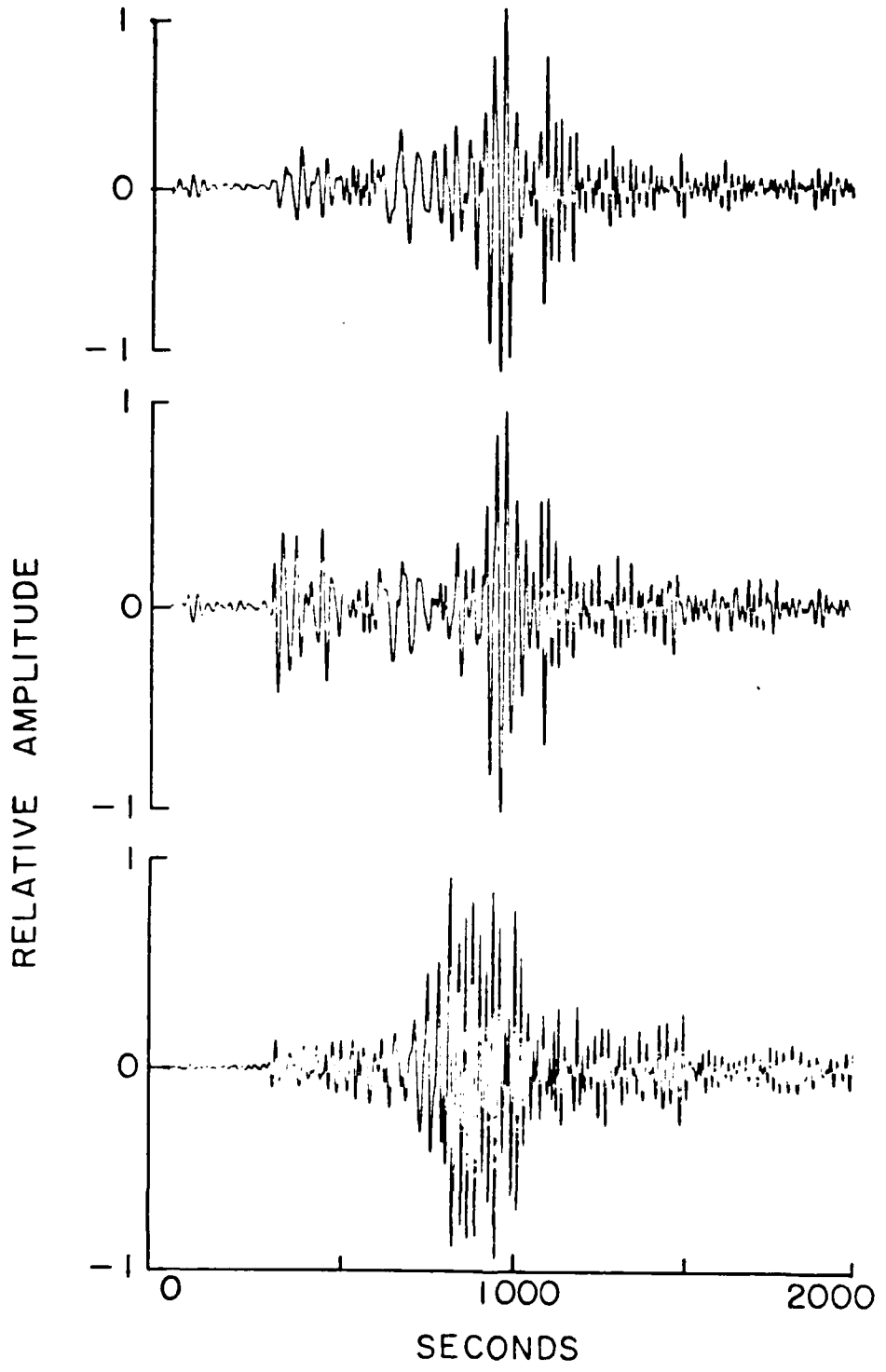

Fig. 1. Surface wave paths (triangles are earthquakes, circles are SRO stations).

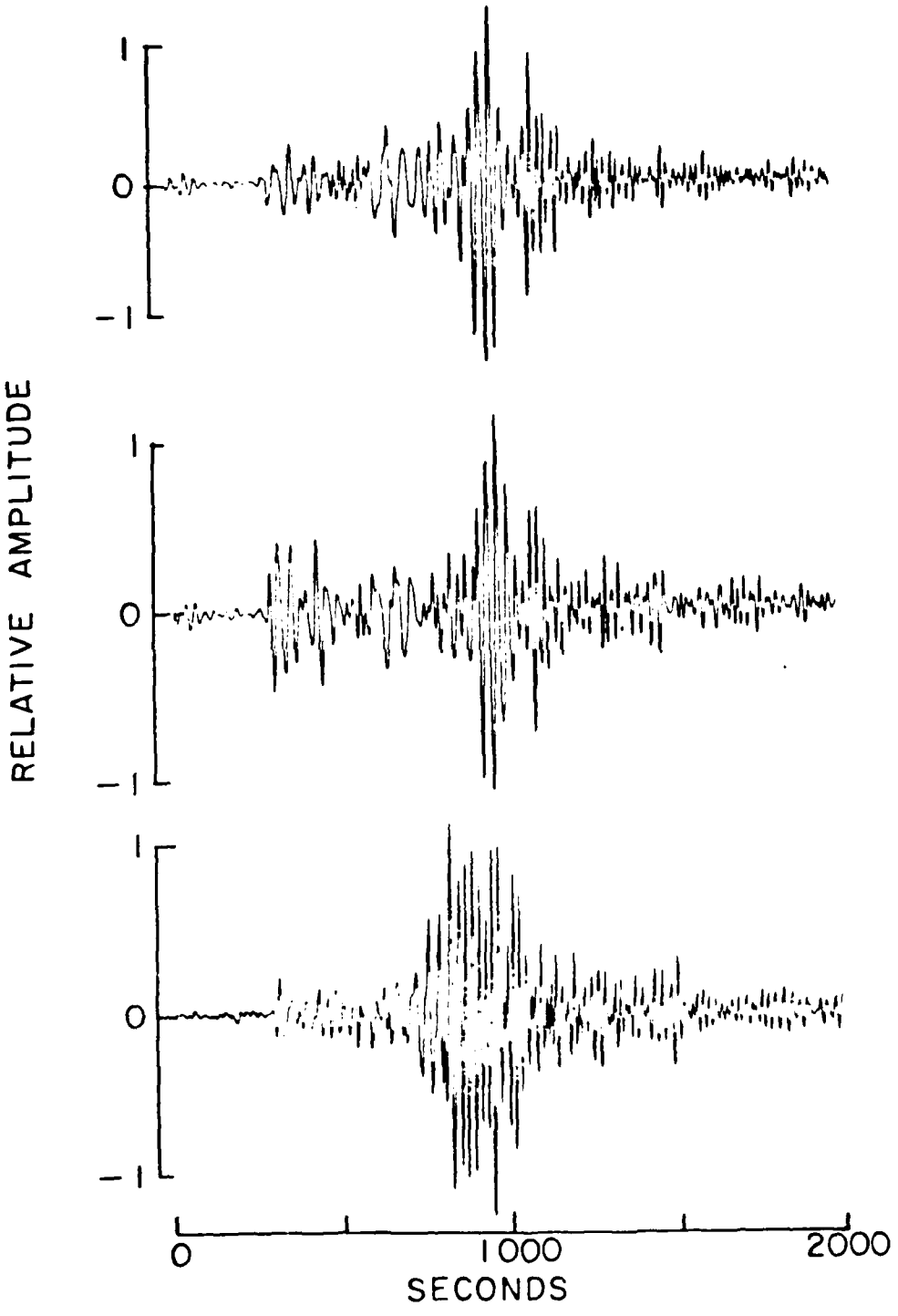

Fig. 2. Unrotated seismograms for the path Yunnan-Mashad, July 3, 1976 (from top to bottom: vertical, NS, and EW).

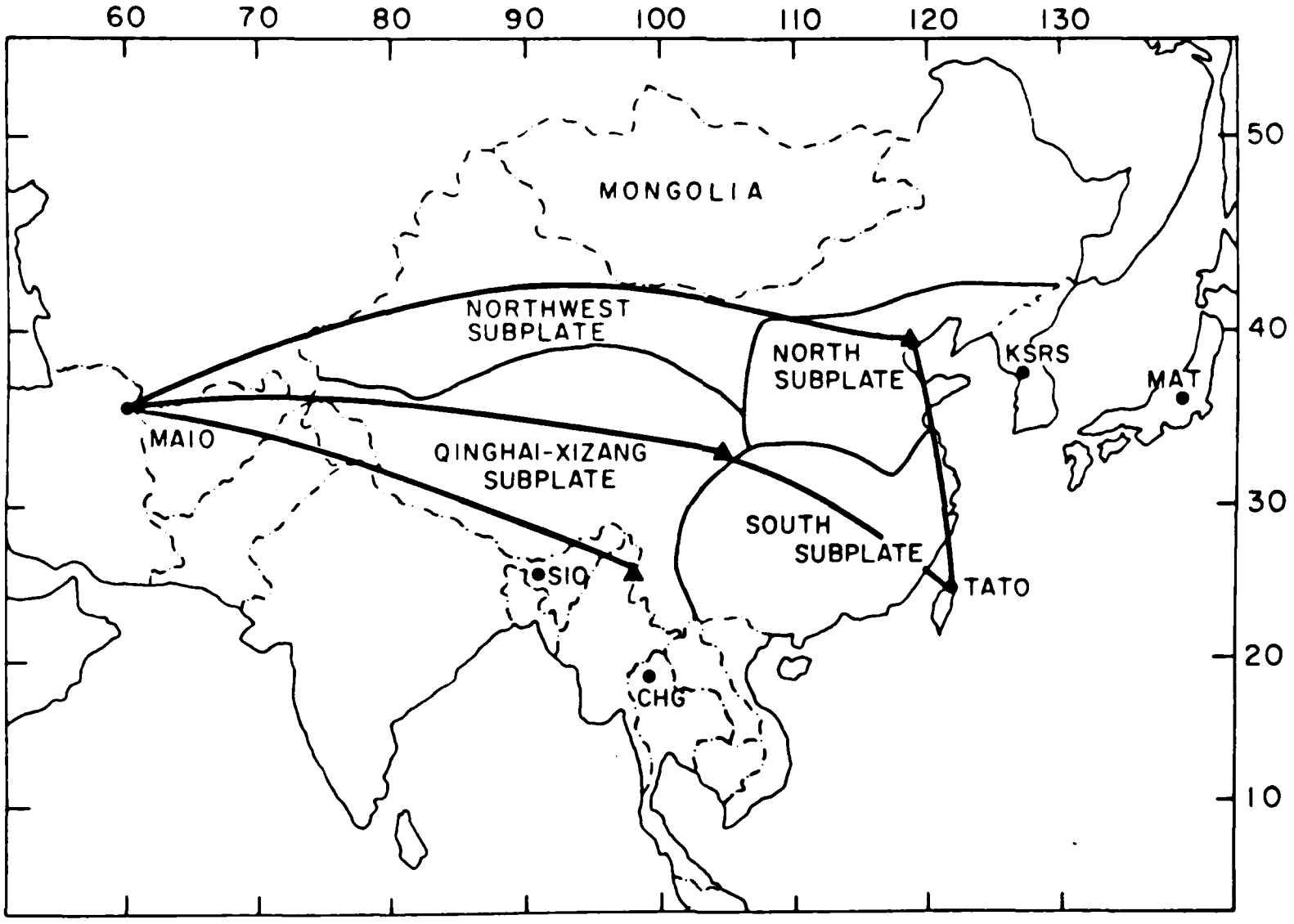

Fig. 3. Rotated seismograms for the path Yunnan-Mashad, July 3, 1976 (from top to bottom: vertical, radial, and transverse).

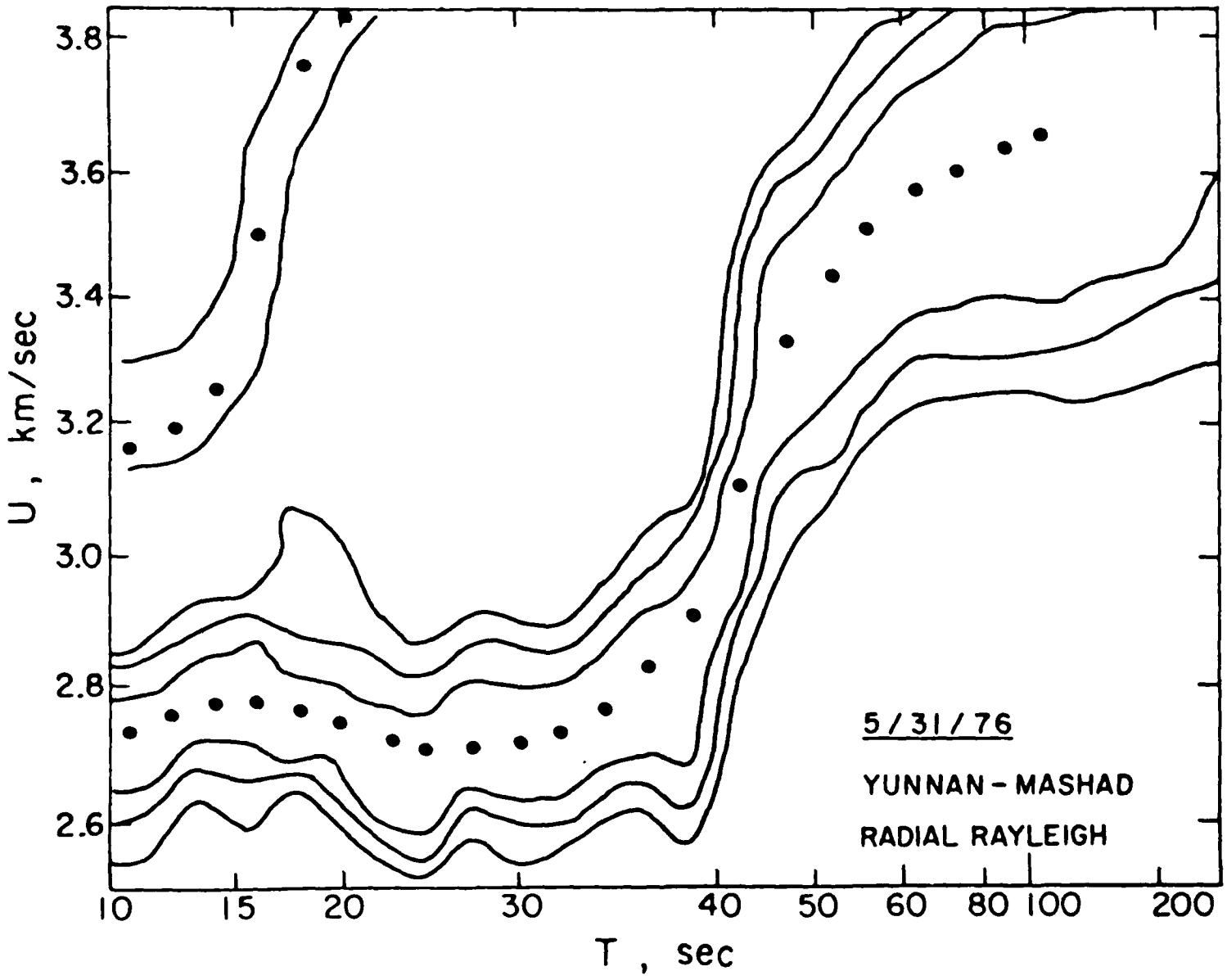

Fig. 4. Results of multiple filtering of Rayleigh wave radial component, Yunnan-Mashad, May 31, 1976.

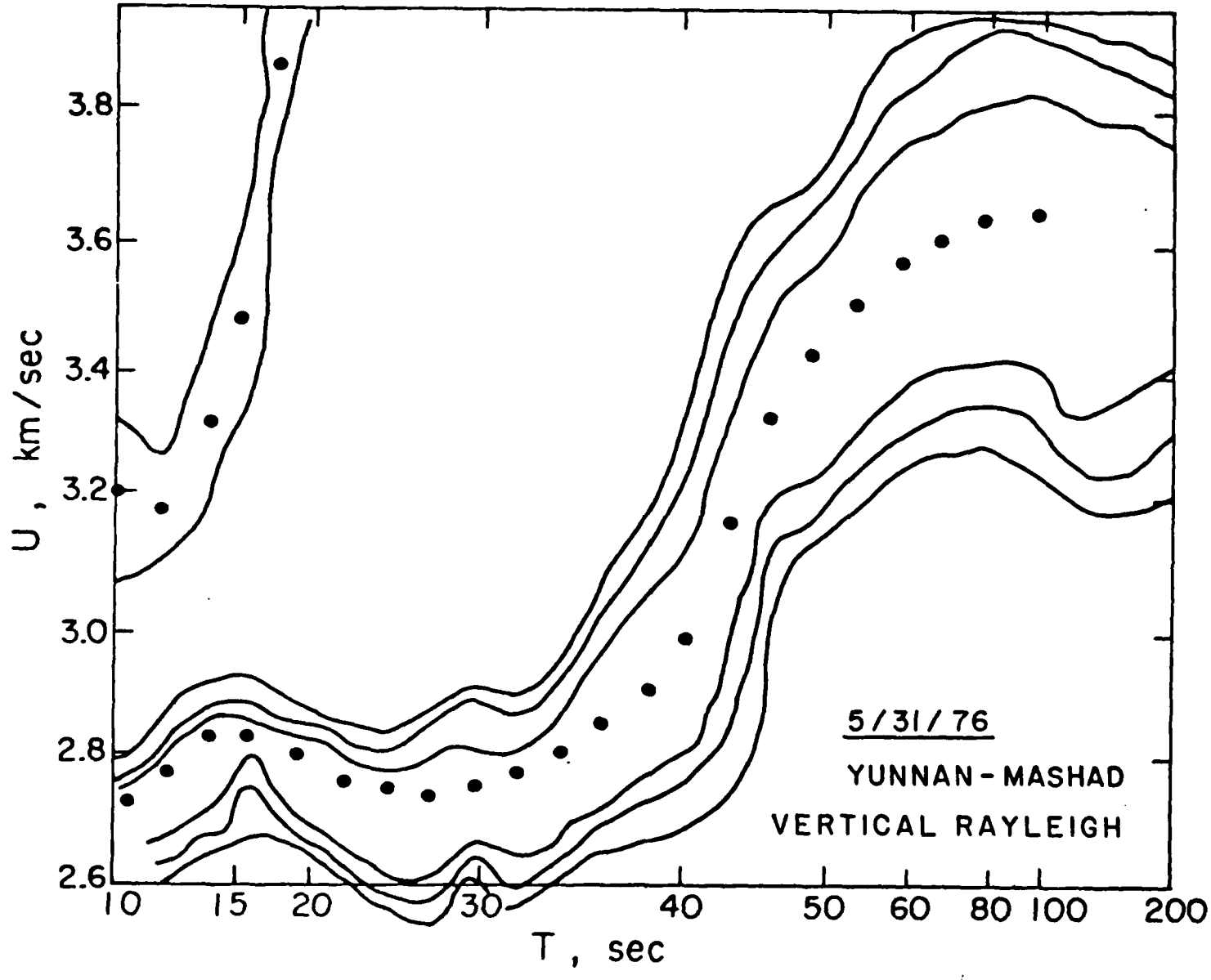

Fig. 5. Results of multiple filtering of Rayleigh wave vertical component, Yunnan-Mashad, May 31, 1976.

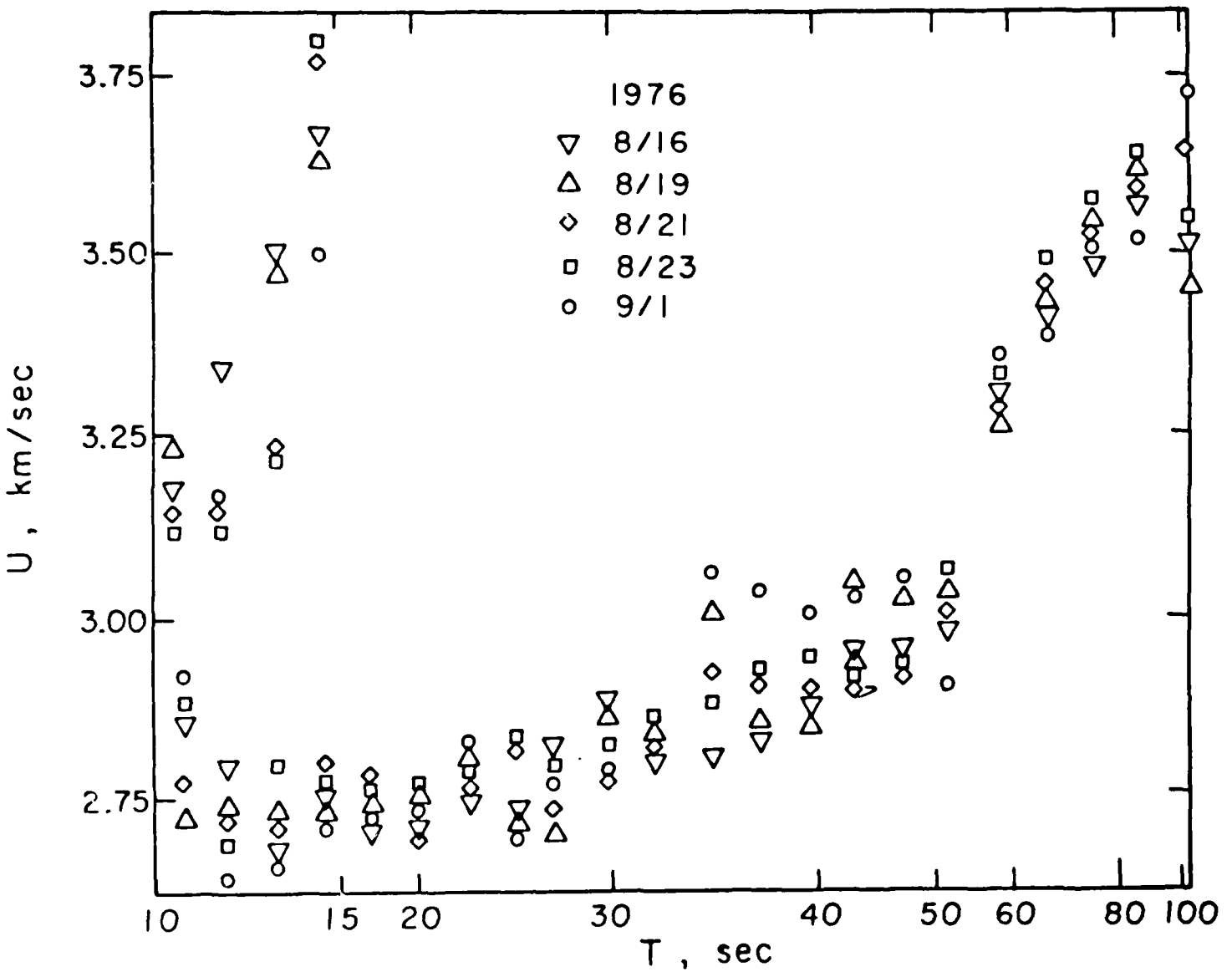

Fig. 6. Group velocity of radial Rayleigh component for five events of the path Sichuan-Mashad.

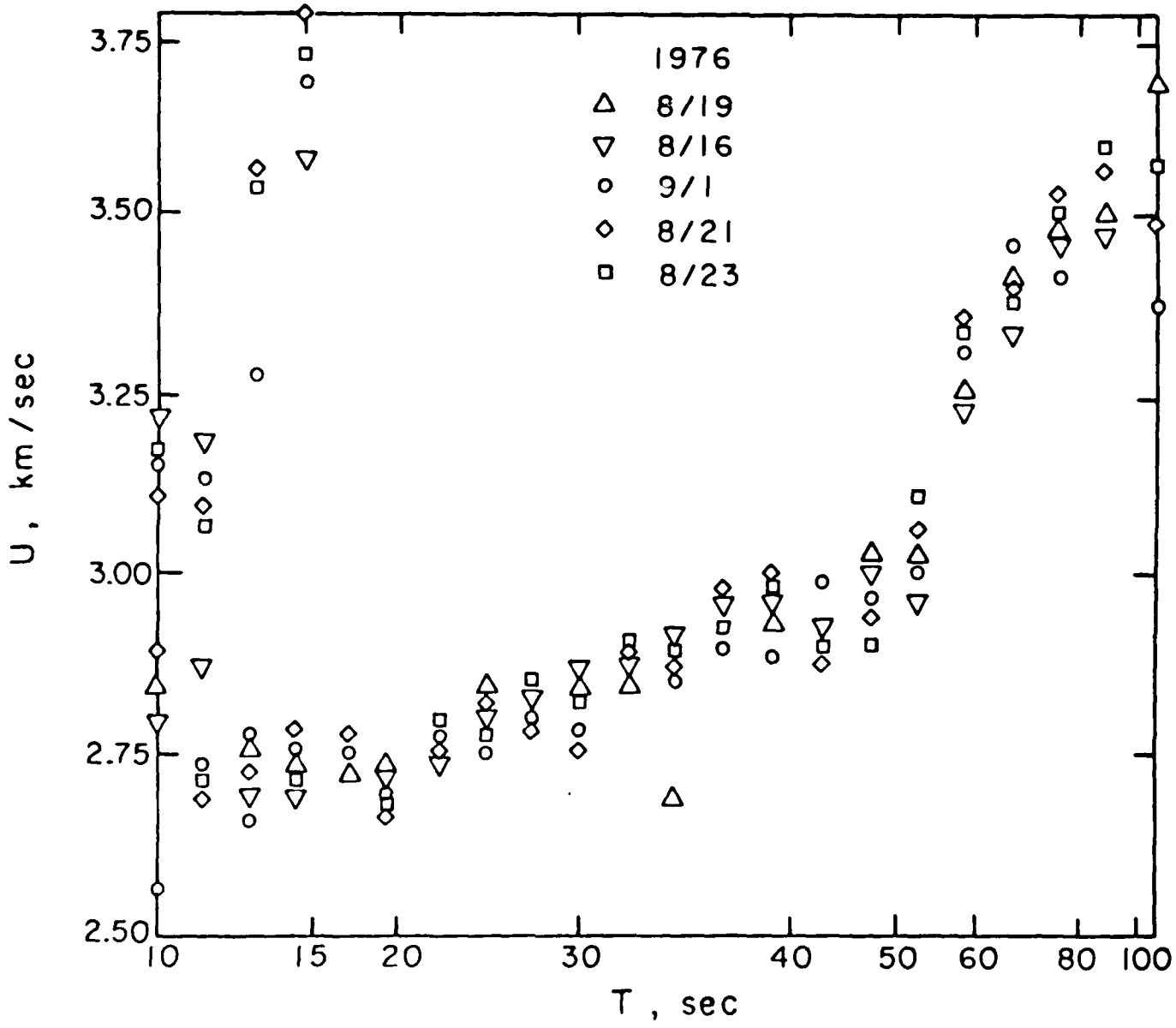

Fig. 7. Group velocity of radial Rayleigh component for five events of the path Sichuan-Mashad.

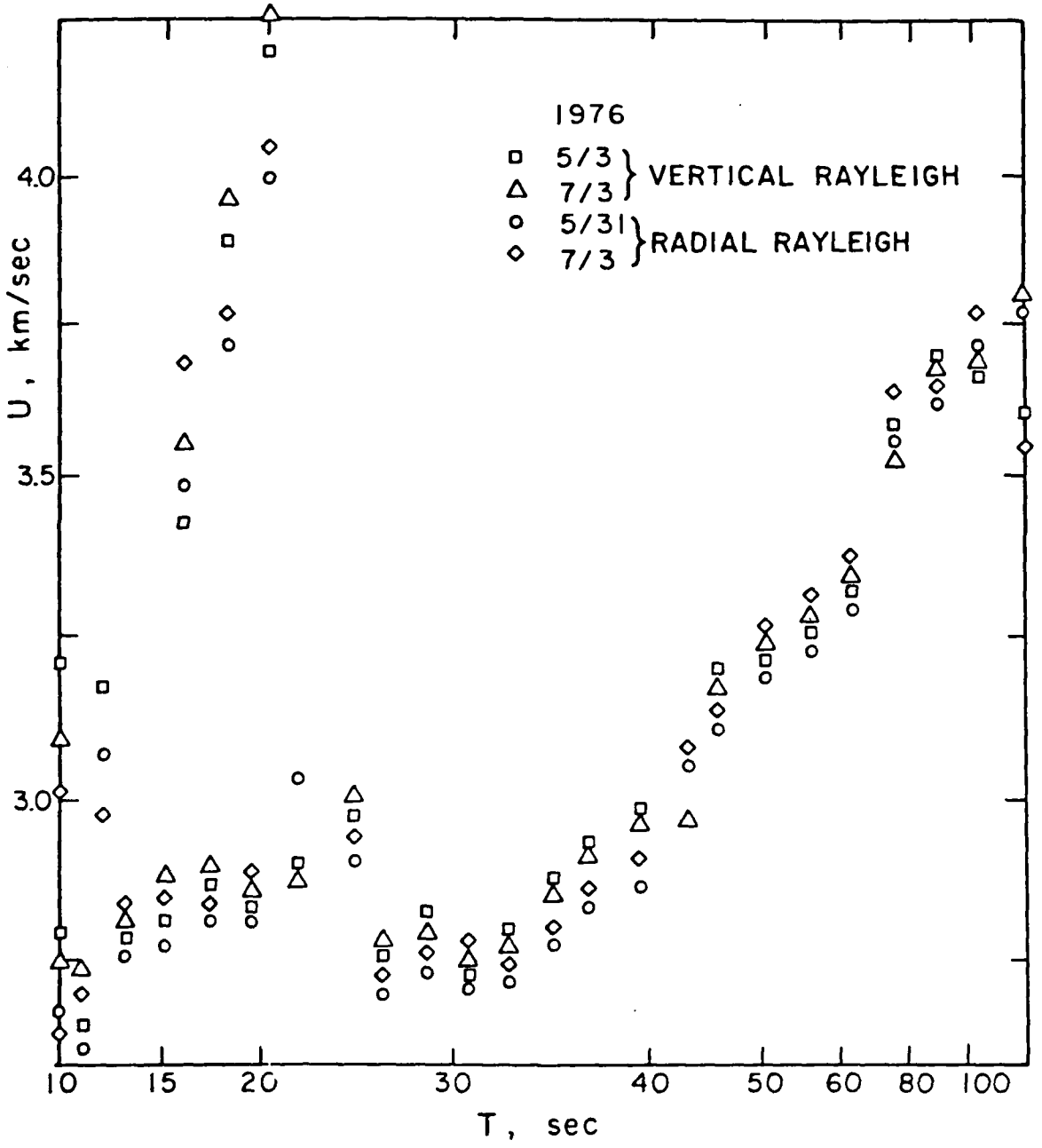

Fig. 8. Rayleigh wave group velocity for three events of the path Yunnan-Mashad.

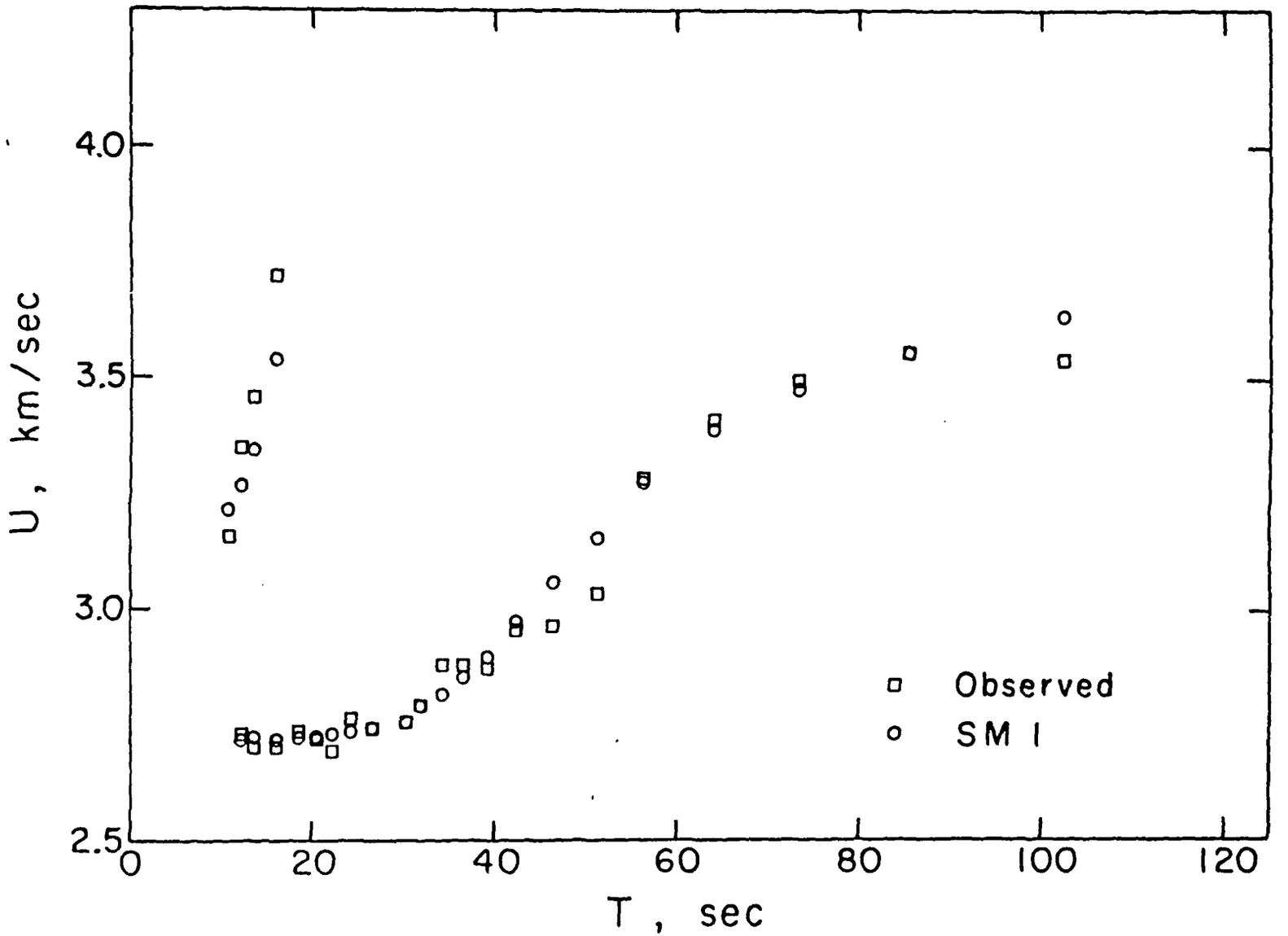

Fig. 9. Theoretical and observed Rayleigh wave group velocities of the path Sichuan-Mashad.

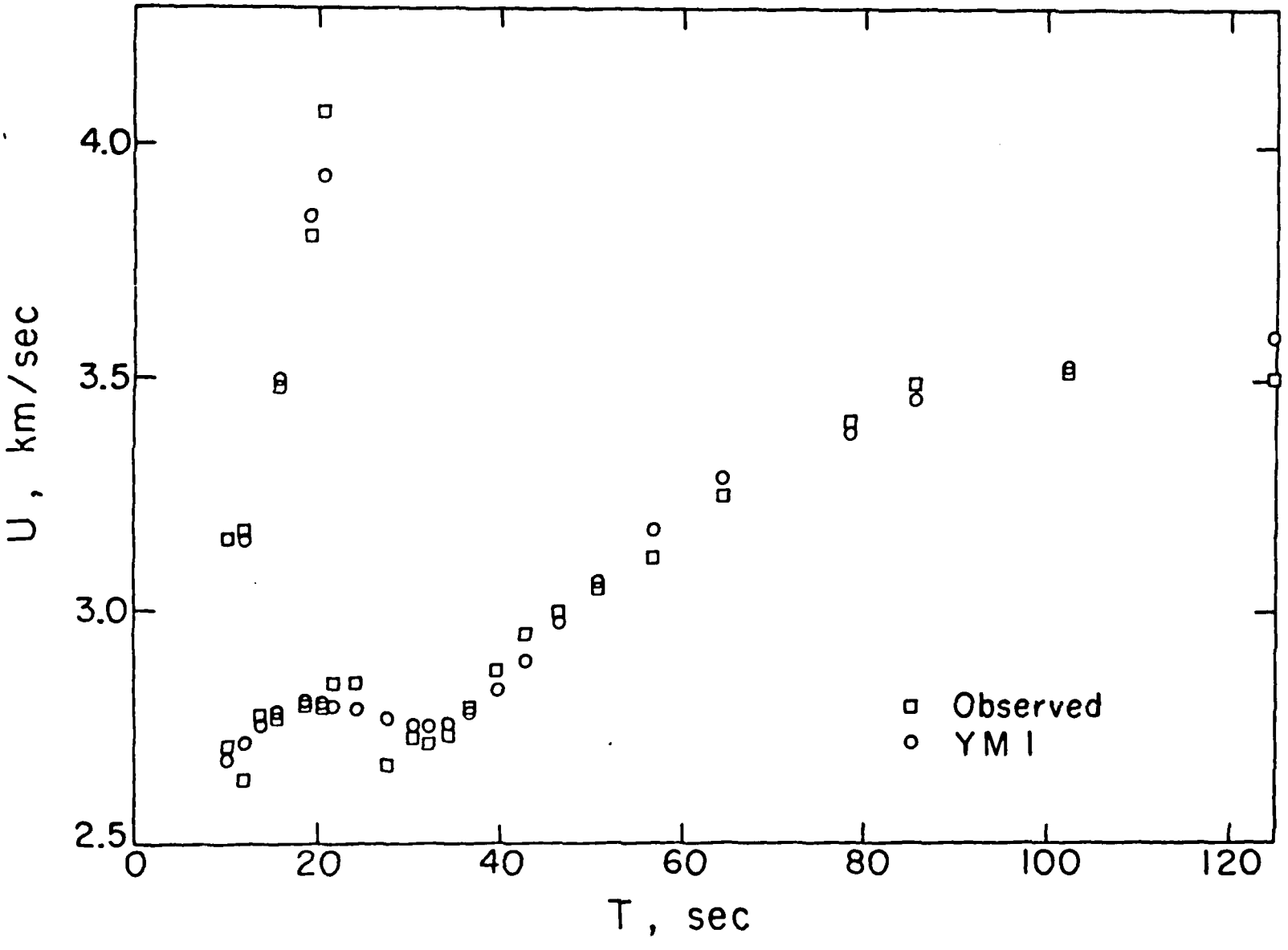

Fig. 10. Theoretical and observed Rayleigh wave group velocities of the path Yunnan-Mashad.

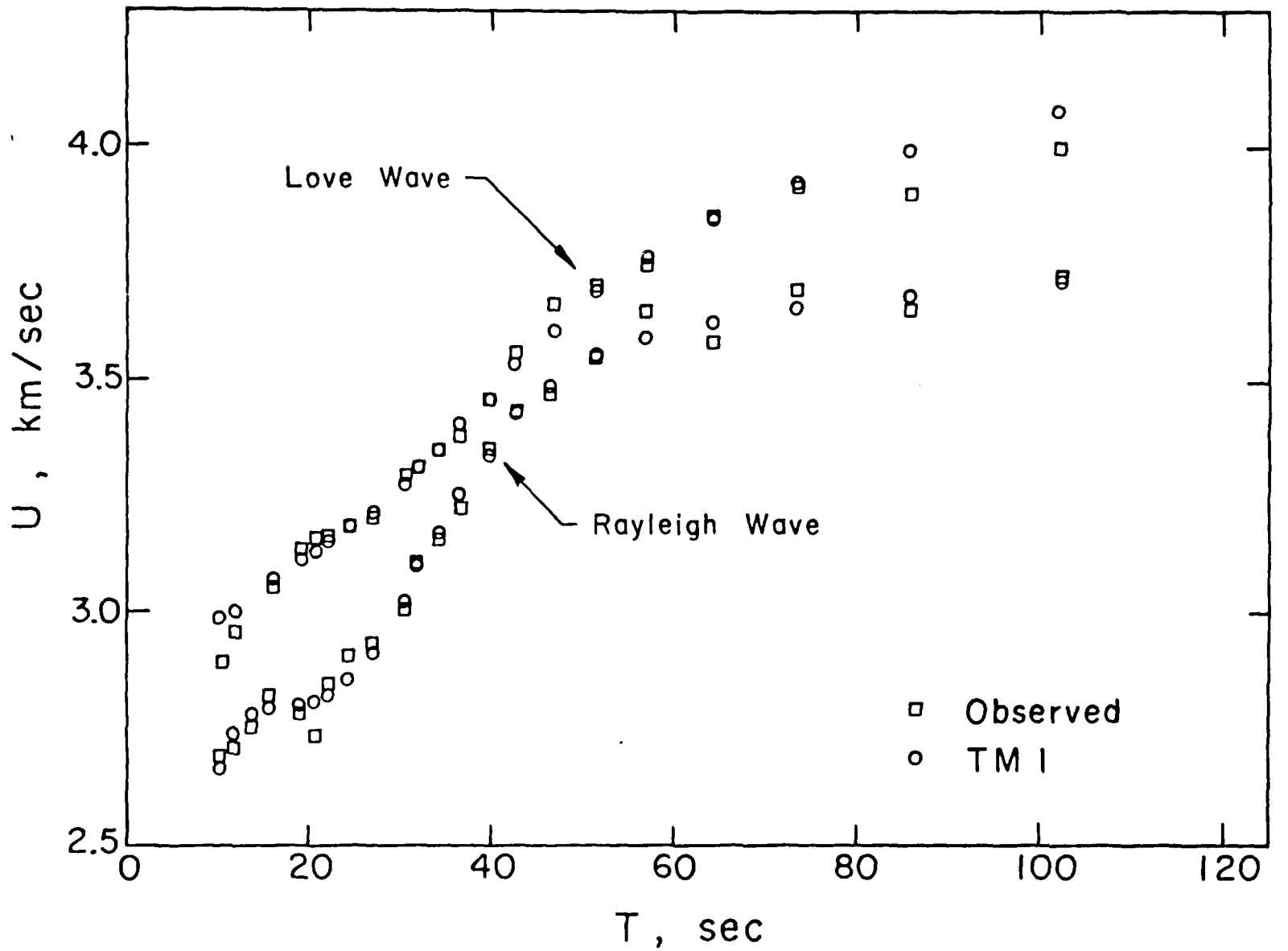

Fig. 11. Theoretical and observed Rayleigh wave group velocity of the path Tangshan-Mashad.

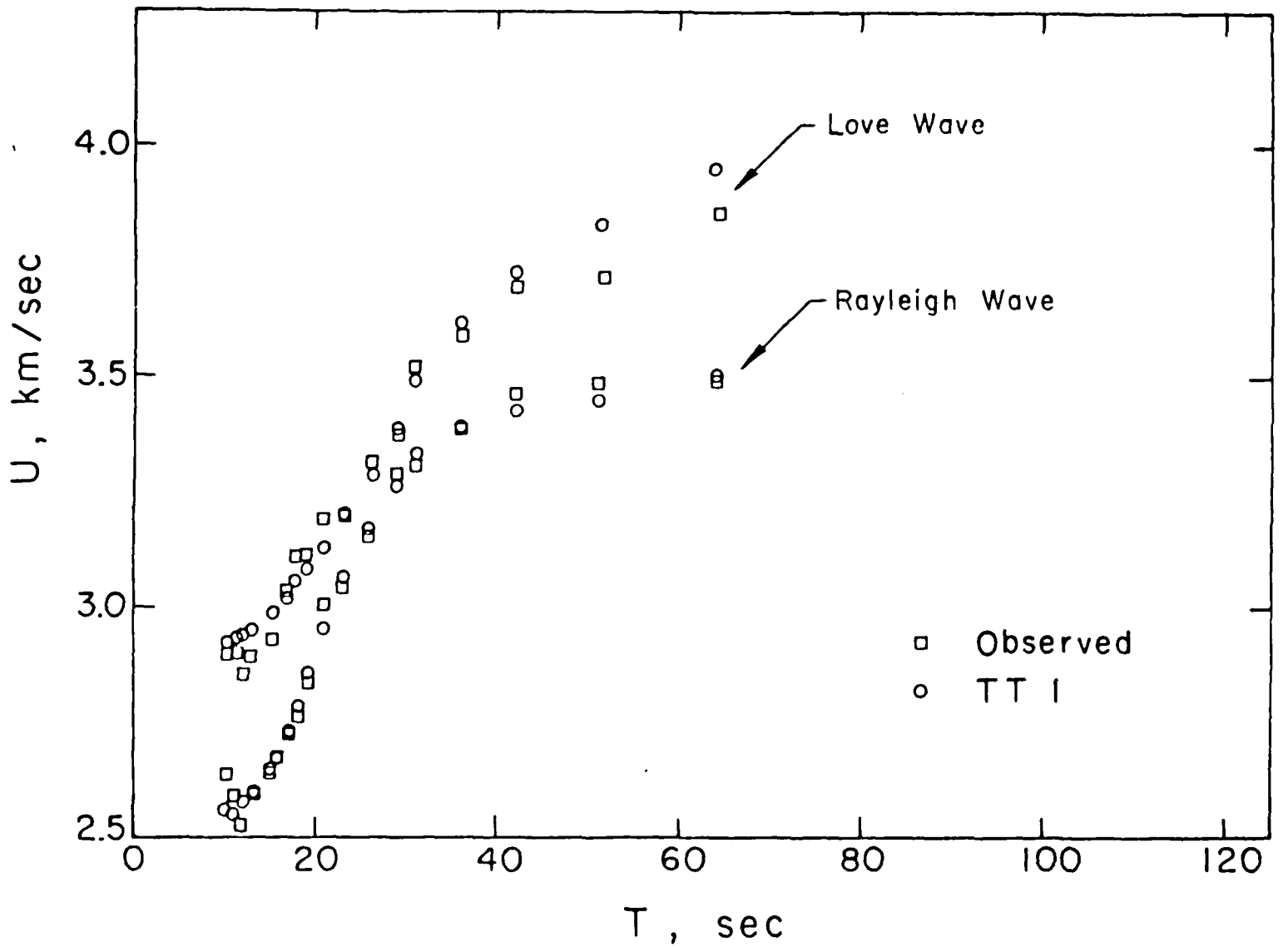

Fig. 12. Theoretical and observed Rayleigh wave group velocities of the path Tangshan-Taipei.

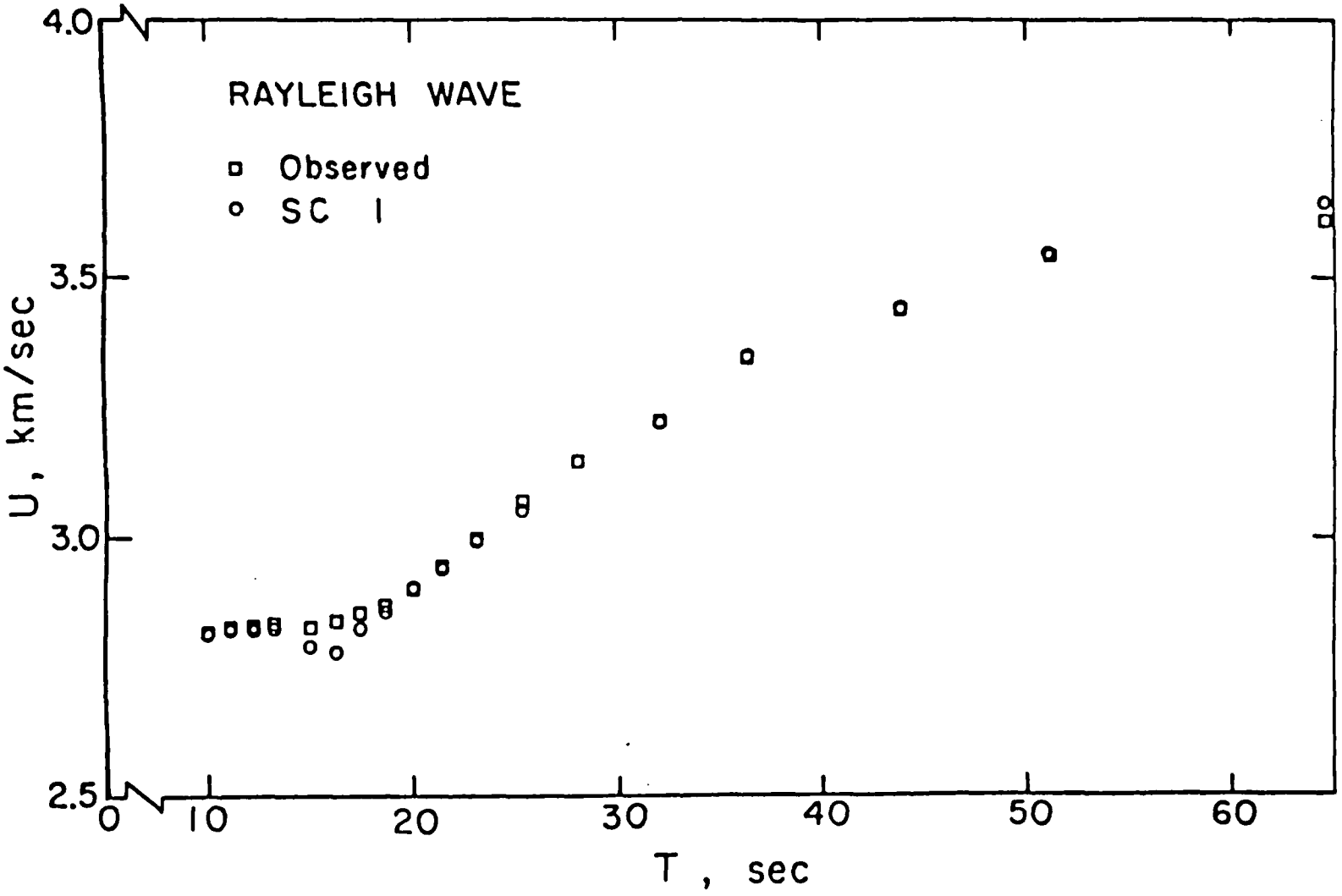

Fig. 13. Theoretical and observed Rayleigh wave group velocities of the path Sichuan-Taipei.

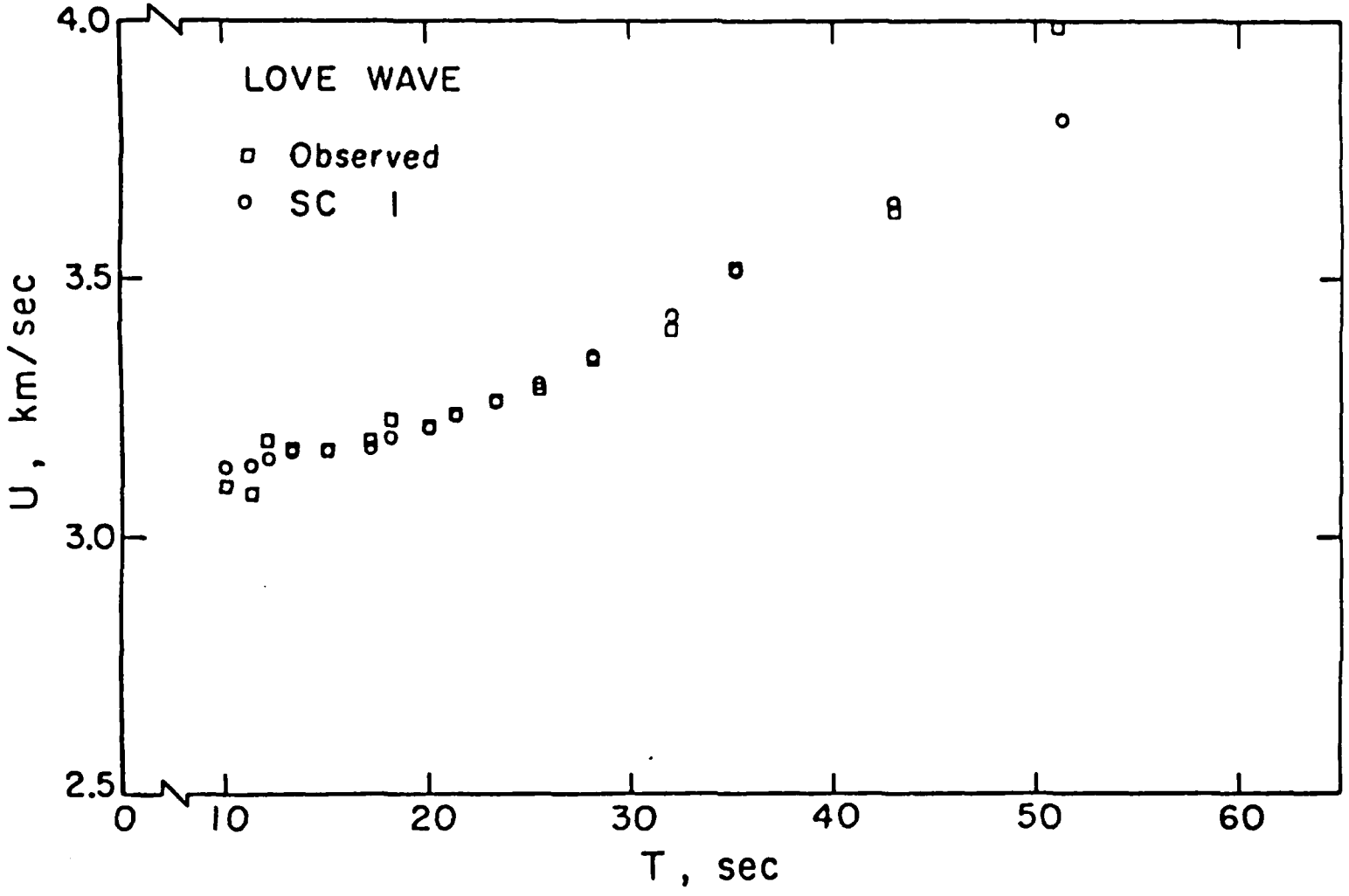

Fig. 14. Theoretical and observed Love wave group velocities of the path Sichuan-Taipei.

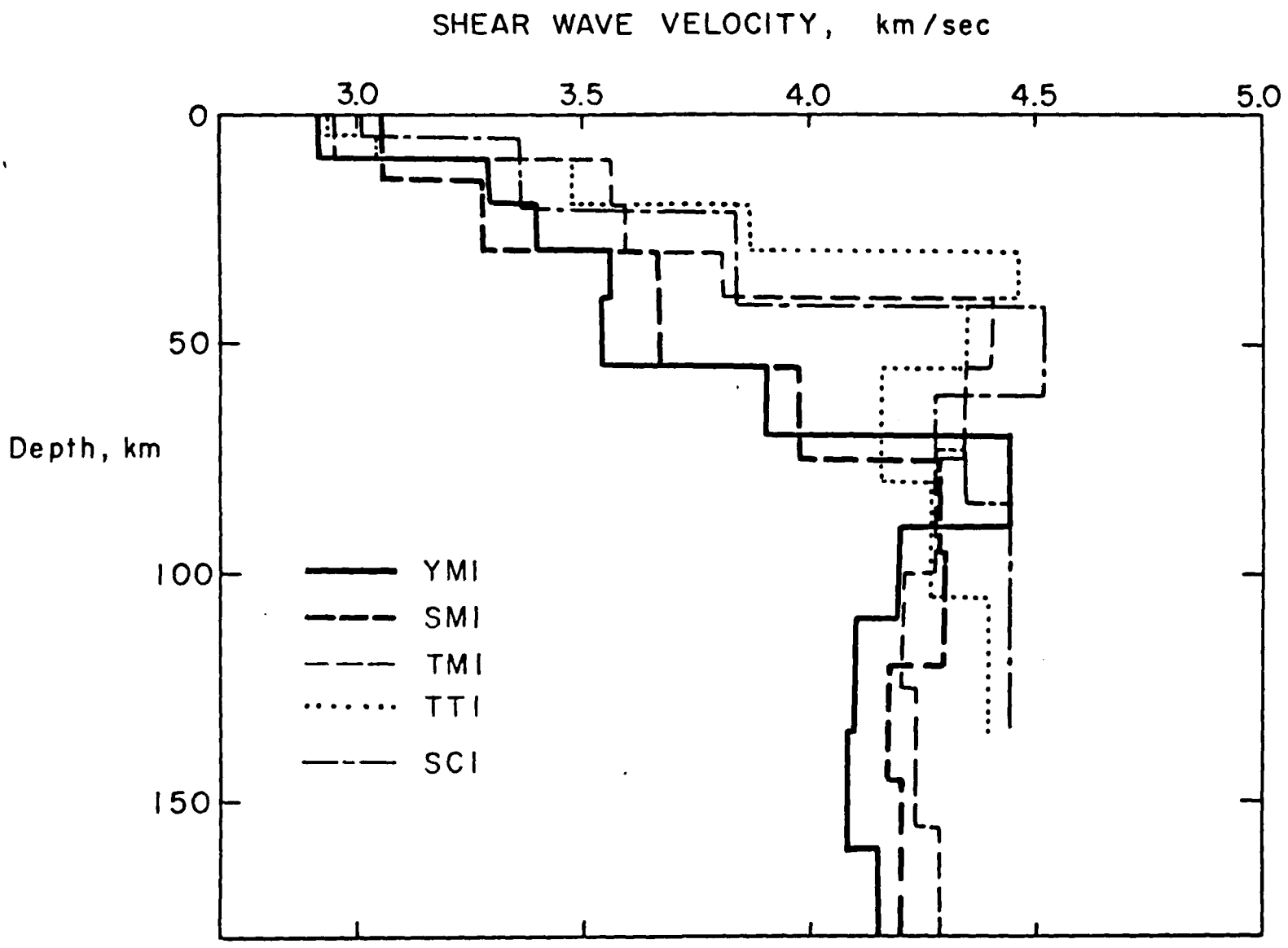

Fig. 15. Crustal and upper mantle structure models for the Qinghai-Xizang plateau (heavy lines) and for the adjacent tectonic provinces (thin lines).